

LUT University
School of Energy Systems
Degree Program in Mechanical Engineering

Antu Datta

LASER INDUCED BIO CELL LYSIS USING PULSED FIBER LASER

Master's thesis, 2019

Updated 10.03.2019

Examiners: Professor, D.Sc. (Tech) Antti Salminen
D.Sc. (Tech) Anna Unt

ABSTRACT

Lappeenranta University of Technology
School of Energy Systems
Degree Program in Mechanical Engineering

Antu Datta

Laser induced bio cell lysis using pulsed fibre laser

Master's Thesis
2019
42 pages, 16 figures, 6 tables

Examiners: Professor, D.Sc. (Tech) Antti Salminen
D.Sc. (Tech) Anna Unt

Keywords: Cell lysis, pulsed fiber laser, plasma, spot diameter, energy density

Dewatering of biosludge is a pre-treatment process for lessening the energy consumption needed for the final disposal. Disrupting the cells for freeing the inside water content can be a solution for dewatering. Laser cell lysis is the process of breaking the cells with the energy of the laser beam. Studies have shown that the plasma creation happening during the treatment acts as the main mechanism in laser induced cell lysis. Laser beam generates plasma during the interaction with the material, which then initiates a shock wave, which is able to penetrate the walls of the cells at certain conditions. This research focused on studying the possibility of plasma formation with the use of a pulsed fiber laser. The intensity of generated plasma and distribution of wavelengths of that was recorded using a spectrometer. Focal point position, processing speed and hatch spacing were varied to compare the changes in brightness of the plasma produced. Focal position had the greatest influence on plasma intensity, as focusing effects the spot diameter of the laser beam on surface of the material and therefore also the power density. At a focal position of +2.0 mm, highest spectral intensity was achieved. Low scanning speed and small hatch spacing brought more energy to the area affected by the pulse and brighter plasma was produced.

ACKNOWLEDGEMENTS

I would like to express my gratitude to everyone who supported me throughout the work. I am grateful for their valuable advice and I am utilizing this opportunity to express my appreciation.

I want to convey my gratefulness to my supervisor Antti Salminen, Professor of Laboratory of Laser Materials Processing in LUT School of Energy Systems, LUT University, for providing me the opportunity to do the thesis work under his supervision, and to Heidi Piili, for valuable advice on carrying out the research.

I would like to express my respect and thanks to my thesis advisor Anna Unt, for being so considerable and supportive throughout the whole thesis work. I am grateful to her, how she has replied to my hundreds of questions and always motivated to do the best performance.

I am grateful to my parents for being supportive in every single moment and to my friends in Finland, who have supported me to stay focused for the studies and for giving me a wonderful time.

Antu Datta

Lappeenranta, 10.03.2019

TABLE OF CONTENTS

1	INTRODUCTION	6
1.1	INTRODUCTION OF THE THESIS TOPIC	6
1.2	BACKGROUND AND MOTIVATION	7
1.3	RESEARCH OBJECTIVES	8
1.4	RESEARCH QUESTIONS	8
2	LITERATURE REVIEW	9
2.1	AIM AND PURPOSE OF THE LITERATURE REVIEW	9
2.2	TERMINOLOGY USED IN LASER LYSIS	10
2.3	MECHANISM OF LASER INDUCED BIO CELL LYSIS	12
2.4	MECHANISM OF PLASMA FORMATION	13
2.5	DEVELOPMENT OF LASER INDUCED BIO CELL LYSIS	14
2.6	PULSED LASERS FOR CELL LYSIS	15
2.7	LASER TYPES USED IN LASER LYSIS FROM LITERATURE STUDY	16
2.8	STATE OF THE ART FOR PREVIOUS RESEARCH.....	17
3	EXPERIMENTAL.....	21
3.1	AIM AND PURPOSE OF THE EXPERIMENTS	21
3.2	EQUIPMENT.....	21
3.3	MATERIAL	25
3.4	EXPERIMENTAL PROCEDURE	26
3.5	PARAMETERS	27
4	RESULTS.....	31
4.1	EFFECT OF THE FOCAL POINT POSITIONS	31
4.2	EFFECT OF THE SCANNING SPEED	33
4.3	EFFECT OF THE HATCH SPACING.....	35
5	DISCUSSIONS & CONCLUSIONS	37
6	FUTURE WORK RECOMMENDATIONS	38
	REFERENCES	39

LIST OF SYMBOLS AND ABBREVIATIONS

D_o	Output beam diameter
D_i	Input beam diameter
E	Energy density
h	Hatch spacing
L	Focal length
P	Effective laser power
v	Scanning speed
λ	Wavelength

1 INTRODUCTION

1.1 Introduction of the thesis topic

Biosludge is a waste product of many industrial processes including wastewater treatment of pulp and paper production. Biosludge has slurry-like consistency and is made up of water and microbial mass. Water makes up over 95% of the total weight of the biosludge. (Yin et al 2004, p 337-348) 5% to 25% volume of the municipal produced wastewater is biosludge (Mowla, Tran & Allen 2013, p. 365-378).

Most of the water is bound within the cell membranes. Dewatering treatment of wet biosludge is energy consuming and requires several subsequent process steps. Drying or dewatering the sludge before burning it in final stage of waste management cycle is done for maximizing the efficiency of whole process chain of waste water disposal procedure. Dewatering has always been challenging because the outer membranes of the particles lock the water inside of the cell, and, the barrier itself carries a high concentration of electrostatic charge. (Jadhav et al. 2017, p. 1-7)

Understanding the phenomena of cell lysis is important for being able to affect the mechanisms involved in dissolution of internal materials from within the cell. Typically, cells have a protein-lipid bilayer, which separates the inner contents from the external surrounding environment. Animal cells have membranes acting as the barriers, but plant cells are surrounded by additional rigid cell wall along the membrane. Plant cell membranes are significantly more durable, and higher effort is needed to induce the damage necessary for cell lysis. (Shehadul, Aryasomayajula & Selvaganapathy 2017, p. 83)

Currently, biosludge dewatering is performed by applying chemical and mechanical processes. Studies have been carried out to develop processes for cell membrane destruction using different methods, including optical, acoustic, mechanical, electrical and chemical means. Measurements of the dry content after mechanical treatment show that only 6% of inner liquids could be removed, which is a very low success rate taking in account the energy expenditure of the process. Alternatively, using sonication for acoustic cell lysis is more time

consuming and along with degradation of the cells excessive heat is being generated. (Brown & Audet 2008, p. 131-138)

Cavitation leading to the cell wall breakage may be induced also optically, using the energy of the laser beam to initiate microscopic shockwaves at the irradiated location. Changes of temperature and physical phenomena involved cause cells to rupture because of rapidly increased shear stress introduced by propagation of shock wave of cavitation bubble. Applications of laser cell lysis have been primarily in field of medical treatment of tumours and assisted drug delivery where it is crucial to keep light induced damage localized. (Sklar et al. 2014, p. 249-262) Process of cell lysis by laser has been shown to be effective, however for making it applicable on industrial level further research is needed.

1.2 Background and motivation

Biosludge from forest and paper production contains high amount of water. The disposal of the biosludge takes high amount of energy because of the water that is remaining locked within the cells and cannot be removed by applying pressure. Laser technology has been developing at considerable pace in recent decades and has become widely accepted manufacturing technique in many industries. Laser as a tool is known for its accuracy and being a non-contact process. Lack of tool wear and other unique features have shown to be practical in biological and medical fields as well. However, using it for cell disruption in industrial scale have not been reported at the time of carrying out of this thesis work. Laser treatment may potentially be suitable to aid with destruction of the cell membranes and therefore freeing the water contents so that the final utilization of the matter by burning would be less energy consuming.

1.3 Research objectives

This work aims to study the effect of the pulsed laser radiation on biosludge substrate with the attention on conditions affecting the plasma formation. Understanding the cell disruption mechanism will be helpful in development of practical arrangements for reducing energy consumption of biosludge dewatering.

The research focusses on the interactions of laser beam with the materials (water and sludge) and observation of plasma formation during the treatment. The methods mainly include comparison of the variations in laser processing parameters and characterization of their influence on the occurrence and intensity of the plasma.

1.4 Research questions

The main point for this research is to characterize the formation of plasma due to water and laser beam interaction and the effect of plasma formation on the bio cell lysis. For achieving this goal, following research questions are relevant:

- How is the laser treatment of biomass preformed?
- How does the laser work to induce bio cell lysis?
- How do the plasma formation and shock wave effect the cell lysis?
- What are the required parameters for achieving the cell lysis via pulsed laser radiation?

2 LITERATURE REVIEW

In this chapter, the main target of the research has been narrated. The chapter introduces with the terminologies used in the report. The mechanism of plasma formation and laser induced bio cell lysis are discussed in this chapter. The chapter mentions about the previous researches done by other researchers and the development with the timeframe. In addition, the state of the art of previous researches and the parameters used in their experimental setup are reviewed.

2.1 Aim and purpose of the literature review

Goal of the literature review of this thesis is to give comprehensive understanding of laser induced bio cell lysis system from laser technology point of view. This literature review was carried out based on articles found in Google Scholar and Scopus. From the articles found from the literature search, the number was quite few for the result of laser induced cell lysis. The previous researches were mainly focused on the plasma formation and optical breakdown. So, it was decided to include the publications from 1991 to 2018 and the related results of wavelength dependent plasma formation for optical break down in water to focus on the mechanism of laser induced cell lysis.

Aim of the literature review is to introduce the terms used to describe the processes, the development of laser induced cell lysis process during the period of 1991 to 2018. The characterization of the mechanism of plasma formation and the cell lysis process is explained. The study area covers the methods of pulsing of pulsed lasers, the parameters used in the previous researches and the know-how of some setups how they were planned in some previous experiments.

2.2 Terminology used in laser lysis

Cell lysis is the process of dissolution of membrane of the cell, to make possible the extraction of the intracellular content like acids or proteins. Cell membrane encloses the internal contents of the cell from surrounding environment and performs as a barrier stopping the inner contents from contact with outside. In a cell lysis process, the outer boundary of the cell membrane is either damaged or destroyed partially or completely, depending on the requirements. (Shehadul, Aryasomayajula & Selvaganapathy 2017, p. 83) Small diameter of pulsed laser beam can create a localized plasma, which initiates an outwardly propagating shockwave with subsequent formation of rapidly growing cavitation bubble. Focal point position and pulse energy effect the threshold energy for plasma formation.

Figure 1 shows the destruction of cell wall and the resulting dissolution of the membrane. As the cell wall is broken, the inner contents can migrate out of the cell.

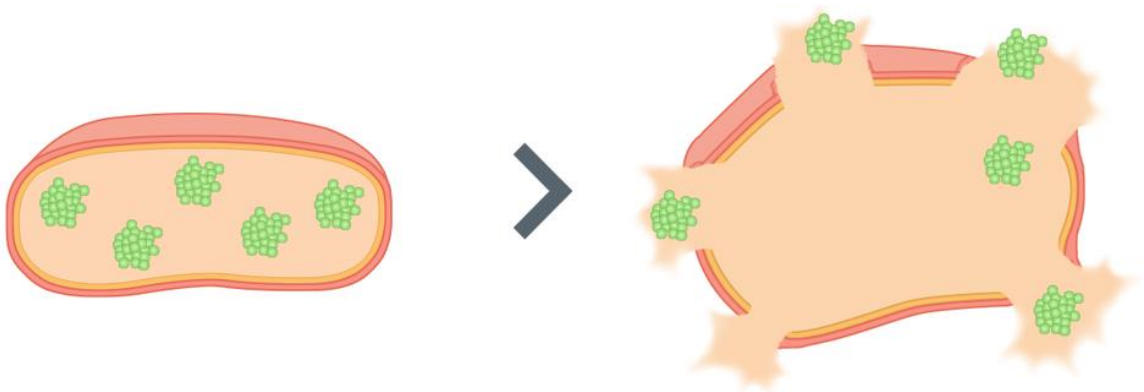


Figure 1. Schematic depiction of cell lysis (Theory.labster.com).

Cell disruption is a method of interrupting the continuity of the cell wall through disorderly outburst which results in release of the inside matter from a cell. Both terminologies mean the same procedure.

Figure 2 shows the cell disruption process where the cell wall is being destroyed by shear stress induced by high pressure and the subsequent release of inner protein molecules.

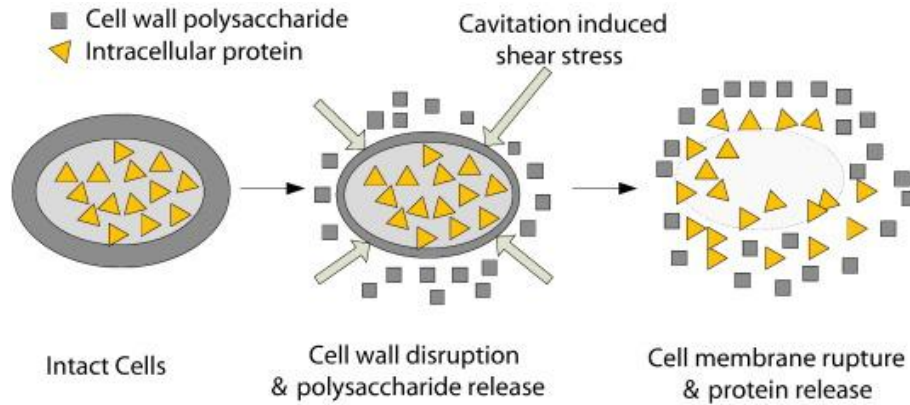


Figure 2. Schematic depiction of cell disruption during ultrasonic treatment due to shear stress and damage of cell wall (Wu et al. 2015, p. 59-65).

Laser lysis is the method of cell membrane destruction by the heat induced from a laser beam. Upon beam meeting the material surface, plasma is created and thereby cavitation bubble is formed. In laser lysis, the cell membranes are destroyed by thermolysis. (Brown and Audet. 2008)

Laser disruption refers to the process for the destruction of cell membrane using laser beam. The term laser disruption is interchangeable with the term laser lysis and is used by several research groups for process description.

2.3 Mechanism of laser induced bio cell lysis

Laser induced bio cell lysis works in thermolysis process. Laser beam increases the temperature and creates plasma on the treated spot. Localized plasma forms shock wave which is outwardly propagating and generates cavitation bubble. Cavitation bubble expands and then contracts in less than microsecond. Due to the quick change of pressure, the membranes outburst. (Rau et al. 2004, p. 2940-2942; Venugopalan et al. 2002, p. 078103)

Figure 3 depicts the stage wise progression of cell lysis by laser induced optical break down due to the interactions of laser beam and the material.

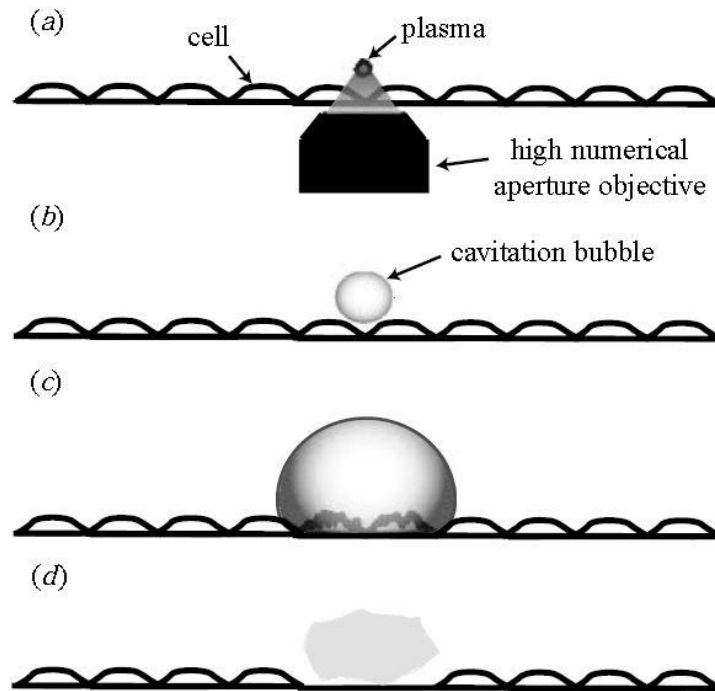


Figure 3. Schematic figure for progression stages of laser induced cell lysis
(Brown & Audet 2008, p. 131-138).

During the laser induced cell lysis, at first stage, plasma is generated due to the laser-matter interaction. Plasma formation increases the temperature at the certain point. Plasma creates shockwave in next stage. The shock wave propagates outwardly and thus there forms vacant space. Cavity bubble is formed at the vacant space. Cavity bubble first expands and within a short time difference contracts and exerts a high amount of pressure.

2.4 Mechanism of plasma formation

Plasma is the fourth state of matter in which; the amount of positively and negatively charged particles is almost the same. Plasma formation is found to be the main mechanism and first stage of cell lysis. Outward propagating shock wave generates cavitation bubble and thus cell lysis occurs. Photoionization, inverse absorption and ionization of particles to provide free electrons form the plasma in transparent liquid and induce the optical breakdown. (Lauterborn & Vogel 2013, p. 67-103)

Interaction of pulsed laser radiation with the surface of the substrate/sample may produce heating, vaporization, melting of plasma formation. Thermolysis process increases the temperature to a very high extent at the interaction place. High temperature results into plasma formation. These phenomena depend on the parameters used and may appear simultaneously. Disassociation of many bonds by a high-powered laser pulse creates a high pressurized and low dense plasma cell and they are interactive with adjacent materials. Intense shockwave is produced by laser-induced plasma, which has impact on the surface and works for the disruption of the particles. Optical penetration depth absorbs the laser energy and increases the surface temperature to a very high extent which causes the formation of vaporization and plasma. As a next step of the process, plasma generates cavitation bubble by propagating outwardly and after a short while the cavity bubbles are contracted. (Mittal & Lei 2018, p. 401) Figure 4 depicts the formation of plasma due to laser beam and material interaction.

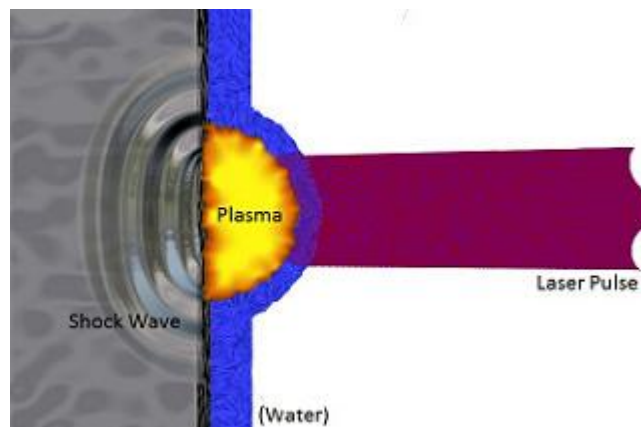


Figure 4. Schematic figure for plasma formation and shockwave generation

2.5 Development of laser induced bio cell lysis

Glezer et al (1997, p. 1817-1819) investigated the use of femtosecond laser pulses for observing the breakdown dynamics of water and shockwave propagation. Lin et al (1999, p. 963-968) visualized cavitation bubble formation within a timescale of 0.1 – 1 micro second, while using nanosecond laser beam for cell lysis. Schaffer et al (2002, p. 196-203) investigated laser lysis by femtosecond laser pulses and used time resolved imaging method for monitoring the optical breakdown induced by laser beam in water. In the experiment, the formation of plasma and dynamics of plasma expansion were observed. Dhawan, Wise & Baeumner (2002, p. 421-426) developed a bio cell lysis system using laser induced disruption method. Rau et al (2004, p.2940-2942) investigated the physical mechanisms of laser induced bio cell lysis and plasma formation was found to be the main mechanism for cell disruption. No effect was observed without the formulation of plasma. Watanabe et al (2005, p. 185-191) observed a permanently damaged region in the cell by focusing femtosecond laser pulses inside the cells. Rau et al. (2006, p. 317-329) examined the use of pulsed laser for bio cell lysis and recorded the formulation of plasma, shock wave and cavitation bubble. Hellman et al (2007, p. 24-35) used frequency doubled and Q-switched Nd: YAG laser (wavelength was 532 nm) and compared the disrupted regions in cells by varying the focal point distance. Lai et al (2008, p. 113-121) demonstrated the method of laser induced cell lysis and investigated the required threshold energy for the optical breakdown.

2.6 Pulsed lasers for cell lysis

Pulsed laser corresponds to the system in which the beam provides the power in a repetitive style. Pulsed laser is suitable to use where higher energy is needed in a time interval. The pulse repetition frequency can be controlled so a high amount of energy production is possible with a longer time frame interval.

Q switching creates the shortest possible pulse duration for a certain pulse energy where nonlinear optical efforts are needed. A loss is introduced by reducing the quality factor inside the resonator. This loss mechanism is replaced when the maximum pulse energy is regained. Q switching produces short pulse energy and a high peak power. (Silfvast 1996, p.53-59)

Mode-locked laser creates extremely short pulses in pulse duration range from picoseconds to femtoseconds. Titanium doped sapphire is a suitable material for the medium as it has considerable wide bandwidth to amplify the frequencies of short length pulses. Mode-locked laser is a frequently used tool to maximize nonlinearity effect. Very short pulse duration tends to create high peak power. (Silfvast 1996, p. 53-59)

Nanosecond laser

Nanosecond laser works at ultraviolet spectral region. Q-switch method is used for generating intense short pulses. Solid state bulk lasers are used for high pulse energy pulsing and fiber lasers are used for small energy pulsing with nanosecond laser. But combining fiber amplifier, fiber laser can generate high average power. (spie.org 2008)

Picosecond and femtosecond laser

Mode-locked laser is used for generating ultra-short and high frequency light pulses. Regenerative amplifiers or cavity dumped lasers are used for high energy pulsing with picosecond or femtosecond laser. (Nishio et al 2014, p. 92380k)

2.7 Laser types used in laser lysis from literature study

Table 1. Parameters used for experimental setup in previous researches

Authors	Types of laser	Wavelength	Pulse duration	Laser power	Beam diameter	Focal length
Vogel et al. 1996, p. 847-860	Nd: YAG	1064 nm	30 ps			
Lin et al. 1999, p. 963-968	Q switched Nd: YAG, Argon-ion	532 nm 488 nm				
Dhawan, Wise & Baeumner 2002, p. 421-426	Nd: YAG	1064 nm		100 mW	2 mm	75.6 mm
Rau et al. 2004, p. 2940-2942	Nd: YAG	532 nm	6 ns			
Watanabe et al. 2005, p. 185-191	Ti:sapphire	800 nm	150 fs			
Lai et al. 2008, p. 113-121	Nd: YAG	532 nm	750 ps		7 mm	
Mcmillan et al. 2013, p. 128-134	Nd: YV04	1064 nm		10 W	100 μ m	

2.8 State of the art for previous research

Lai et al. (2008, p. 113-121) used a diode pumped, Q-switched Nd: YAG laser (the wavelength was 532 nm and the pulse duration was 750 ps) for the experiment. In the experiment, the beam diameter was optimized using an iris diaphragm to utilize the least threshold energy for achieving the optical breakdown in water.

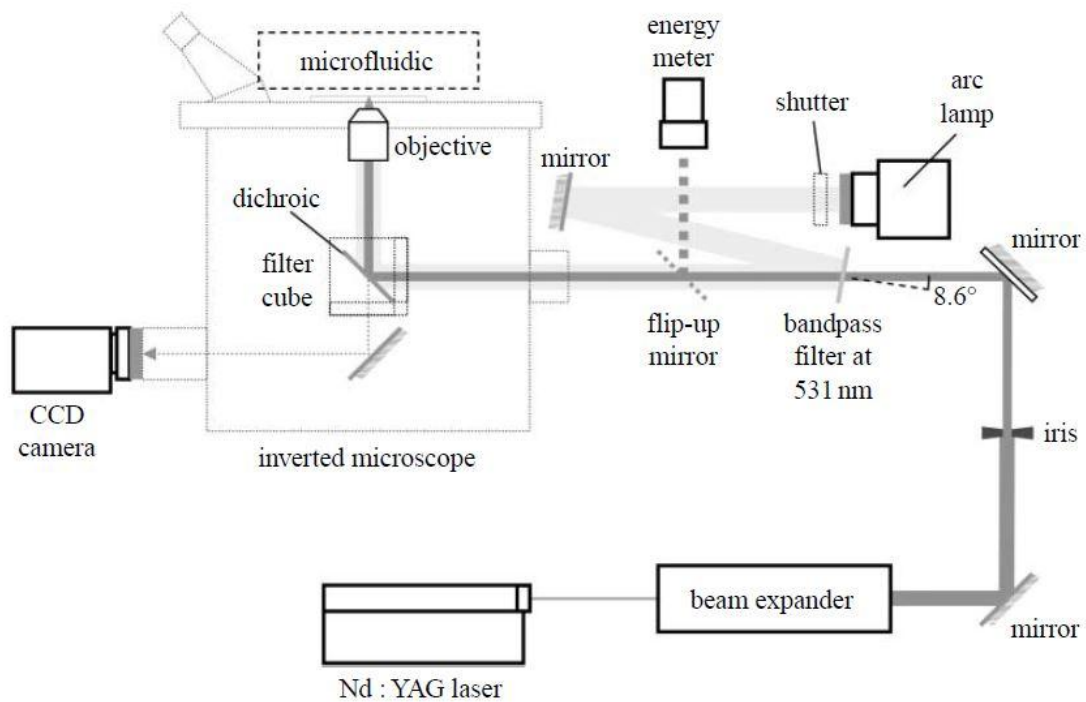


Figure 5. Schematic diagram of the experimental setup used by Lai et al. 2008

The use of pulsed laser microbeam was successful and from the experimental result, the successful formation of plasma due to small beam diameter was observed. The threshold energy for plasma formation was measured by moving the focal point at different locations and the values differed in different positions. In this study, for 6, 13, 19, 25, 38 and 44 μm distance from microchannel bottom, the threshold energy for plasma formation was accordingly 2.5, 2.2, 1.9, 1.8, 1.9 and 2.1 μJ . Lowest threshold energy of 1.8 μJ was recorded at 25 μm and 31 μm . (Lai et al. 2008, p. 113-121)

Watanabe et al. (2005, p. 185-191) experimented for the disruption of mitochondria in living cells. They used a setup combining two laser sources. A He-Ne laser (wavelength 543 nm) and an Ar-ion laser (wavelength 488 nm) were focused on the cell through an objective lens for the visualization of organelles. A regeneratively amplified Ti:Sapphire laser (pulse duration 150-fs and wavelength 800 nm) was used for the irradiation of laser beam.

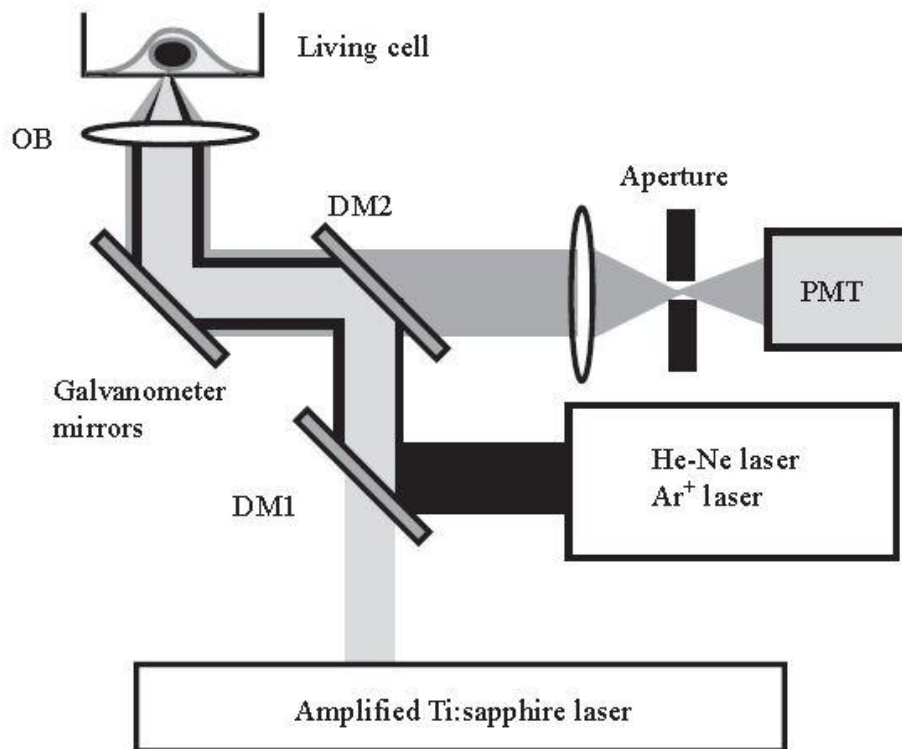


Figure 6. Schematic diagram of the experimental setup used by Watanabe et al. 2005.

The experiment was mainly targeted for single cell mitochondria disruption. The system was effective for desired area in single cell. Cell dynamics studied from this experimental setup is useful for targeted disruption of bio cell membrane.

Rau et al. (2004, p. 2940-2942) studied the cell lysis mechanism with a Q-switched, frequency doubled Nd:YAG laser having 6 ns pulse duration and 532 nm wavelength. Pulse energy was varied from 5.6 μ J to 24 μ J. Studies confirmed that the plasma formation during the process as the cause of cellular disruption. Sample cells did not show any difference without the presence of plasma in the course of laser treatment. In experiments, the plasma

formation was recorded after 10 ns of beam application. During the plasma presence in the process, an outward facing pressure wave was generated which formed a cavitation bubble. The rapid expansion of the bubble induced damage to cell membranes, thus, the phenomena was shown to be a result of optical breakdown caused by laser lysis.

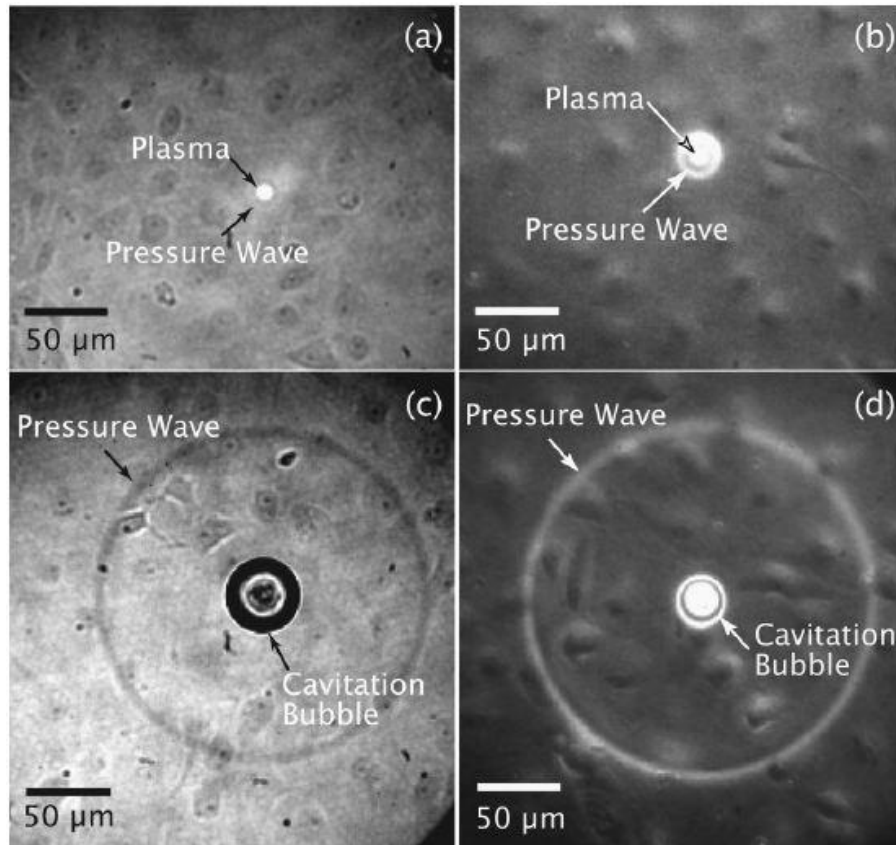


Figure 7. Visualization of laser induced plasma formation (Rau et al. 2004, p. 2940-2942).

Figure 7 Plasma formation during different time duration. (a) and (b) were recorded after 10 ns while (a) was captured using bright field and (b) was captured using phase-contrast microscopy. Cavitation bubble generated by plasma is shown on (c) and (d).

Gazor et al. (2018, p. 49-54) investigated the laser induced cell lysis using *Pichia Pastoris* yeast and continuous wave laser radiation (wavelength 1064 nm and pulse power 284 mW). The process was found to be cleaner and more convenient than conventional cell membrane destruction methods including mechanical, electrical, ultrasonic and chemical. 90% of the cells were disrupted from the total number of cells during the experiment.

Dhawan et al. (2002, p. 421-426) investigated cell lysis with 2000 E. coli cells per sample for different power exposure using Nd:YAG laser. The wavelengths used were from 500 nm to 1550 nm. Wavelength 1065 nm and 1250 nm were most effective for cell lysis when applying 100 mW laser power and resulted in about 50% of the cells being disrupted. Increment of laser power to 200 mW and 300 mW succeeded for the disruption of 80% and 99.8% cells accordingly.

3 EXPERIMENTAL

This chapter provides the details about the equipment, experimental setup and parameters used in the study. The chapter includes information about parameter variation during the experiments.

3.1 Aim and purpose of the experiments

Aim of the experiments was to induce plasma formation and to analyse the spectral intensity of plasma during laser beam treatment of biosludge. The experiments were carried out in the Laser Materials Processing Laboratory of LUT University. The tests included variation of focal point position, processing speed and hatch spacing.

3.2 Equipment

Laser

An ytterbium pulsed fiber laser manufactured by IPG Photonics with a maximum output pulse energy of 1 mJ was used for the experiments. The pulse duration can be controlled from 4 ns to 200 ns and the pulse repetition can be set from minimum 1.6 kHz to maximum 1000 kHz. The wavelength of the beam is 1064 nm. Beam caustics are shown in Figure 8.

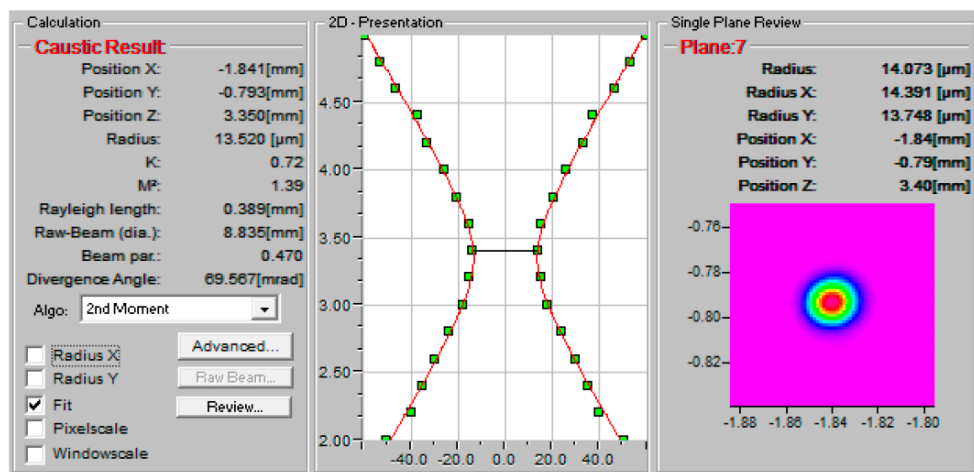


Figure 8. Beam caustics measured with Primes MicroSpotMonitor beam analysis tool

The maximum peak power of the laser is 15 kW and can be adjusted as a percentage of the maximum from 10% to 100%. The laser beam focal point diameter was $\sim 40\text{ }\mu\text{m}$ with a Rayleigh length of 0.39 mm and divergence angle of 69.567 mrad. Laser used in the experimental setup is shown in Figure 9.

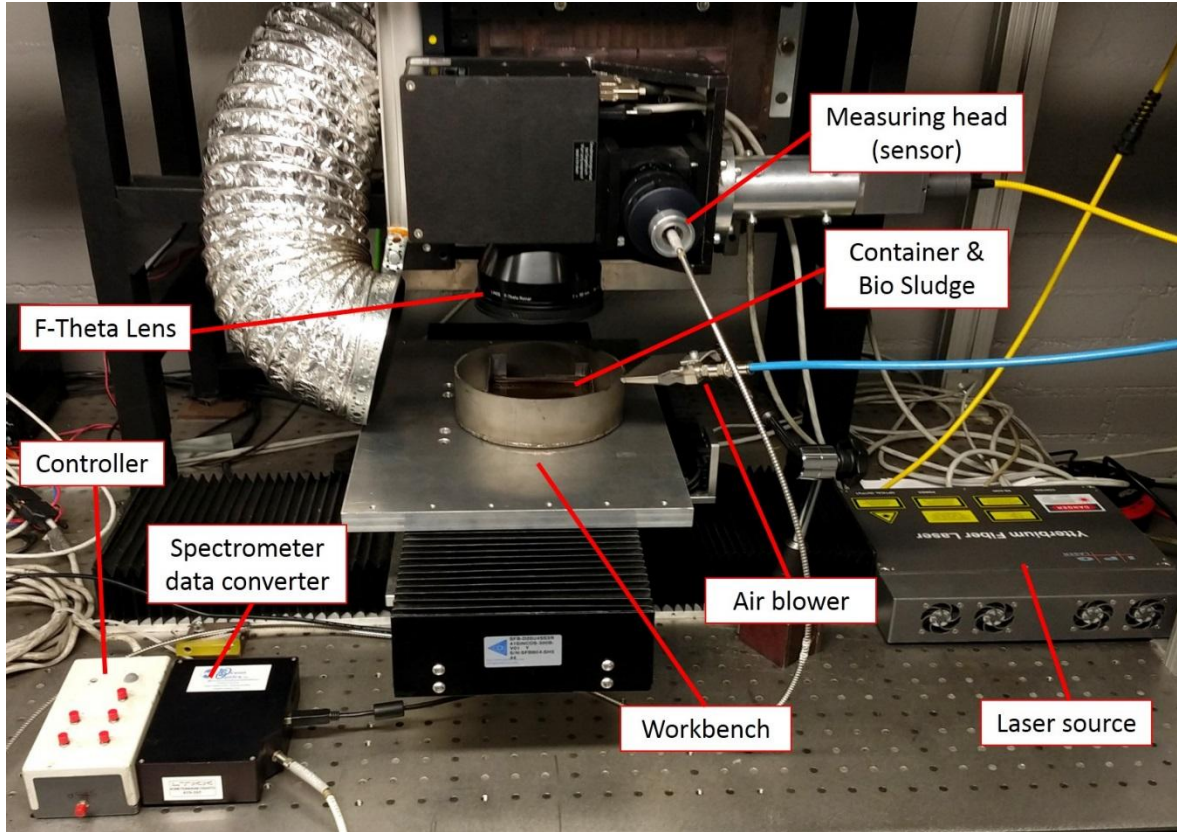


Figure 9. Laser device used for the experiments

The laser system was controlled by a computer through an RTC 4 Interface board. The scanner head controls the mirror movement to move the laser beam in the required path. The scanner head was a Scanlab's Hurriscan 14 II with an f100 telecentric lens. A software named SAMLight was used to adjust the laser parameters and an YLP C-series utility software from IPG was used for varying the pulse duration. Table 2 shows the different parameters of the ytterbium pulsed fiber laser equipment.

Table 2. Specifications of IPG laser device used in the experiments (IPG Laser GmbH 2009).

No	Characteristic	Minimum	Type	Maximum	Unit
1	Mode of operation	Pulsed			
2	Polarization	Random			
3	Selectable pulse durations	4, 8, 14, 20, 30, 50, 100, 200			ns
4	Central emission wavelength		1064		nm
5	Emission bandwidth		5	10	nm
6	Nominal average output power		20		W
7	Output power adjustment range	10		100	%
8	Extended pulse repetition rate	1.6		1000	kHz
9	Maximum pulse energy		1		mJ
10	Maximum peak power		15		kW
11	Laser switching ON/OFF time		2	3	
12	Long term average power instability		2	5	%

Spectrometer

Spectrometer is a device to measure the properties and phenomena of light, including wavelength, energy and frequency, polarization etc. A fiber optic spectrometer of model HR 2000+, manufactured by Ocean Optics was used for the measurement of the spectral intensity of plasma formation by detecting emitted light intensity. The emission spectrum of a light source can be measured in a specific wavelength interval and that is done by changing the exposure time of CCD-array to the light emission source. The spectrometer is responsive to a calibrated wavelength range from 190 nm to 640 nm with a maximum resolution of 0.035 nm. Adjustment of grating and entrance slit, control the allowable range and resolution for the measurement. (Ocean Optics, Inc) Figure 10 shows the spectrometer used in the experiment.

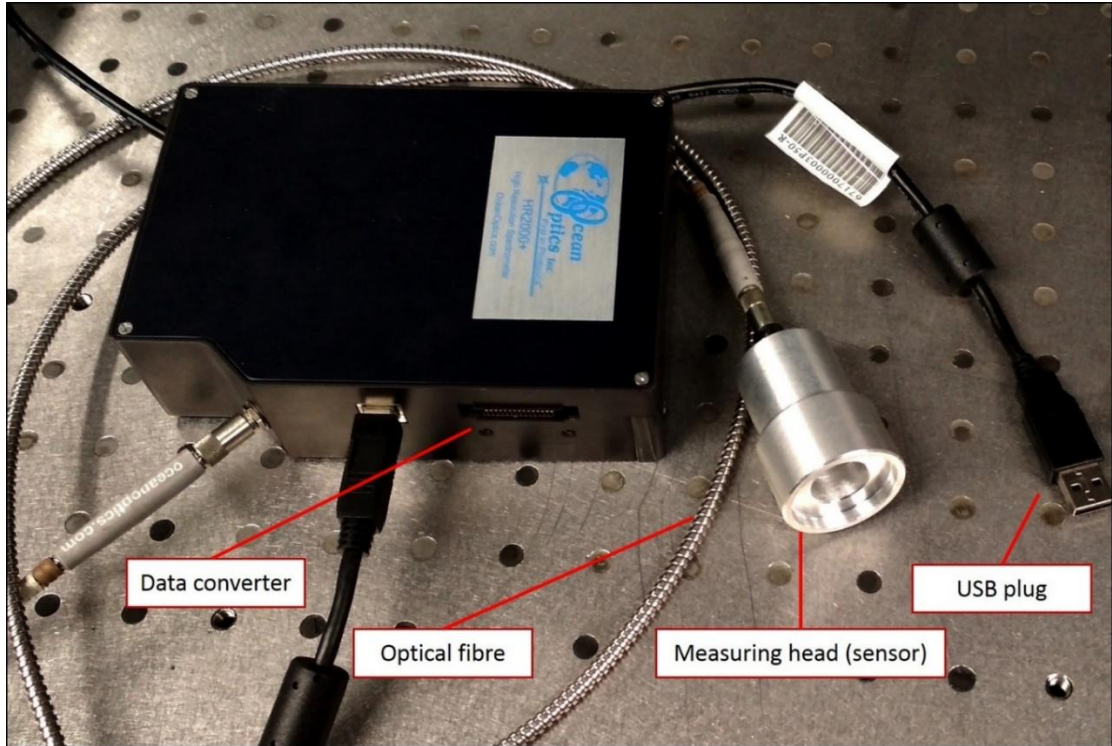


Figure 10. Spectrometer used in the experimental setup

The spectrometry setup consisted of a spectrometer, an optical fiber to send the signal to computer and a detector head. The spectrometer was operated by OceanView software. The spectrometer was directly connected to the computer using a USB port. Therefore, it did not require any external power source and the computer worked as the power source for the spectrometer.

3.3 Material

Biosludge is produced in a high quantity as a waste from pulp and paper industry, which is mainly generated from wastewater treatment. The sludge used in the experiment was a wastewater treatment byproduct from a paper industry. Biosludge contains around 50-80% water and high amount carbon rich substance. The sludge was preserved in the freezing temperature before the experiments.

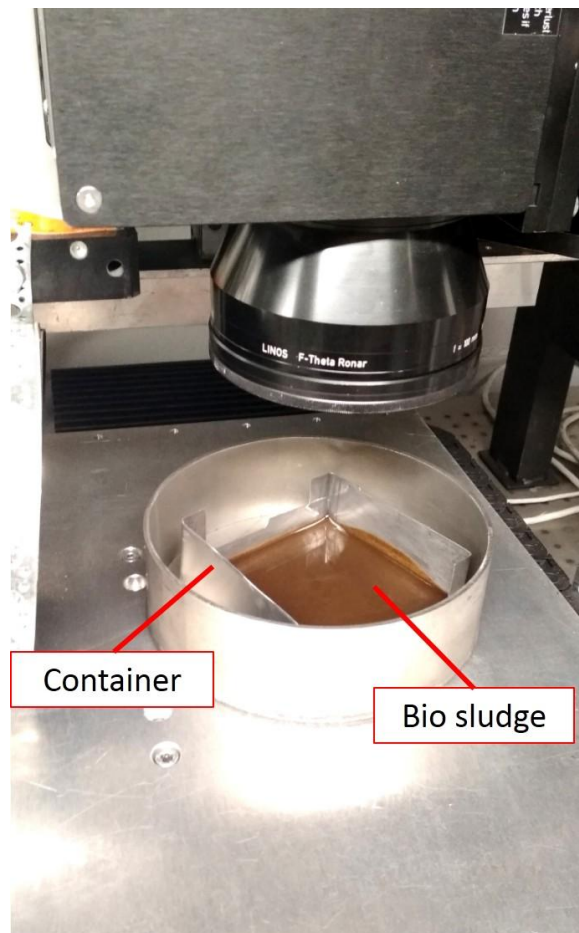


Figure 11. Biosludge used in the experiment

Figure 11 shows the material for the experiment holding in a container for the experimental setup.

3.4 Experimental procedure

Biosludge was poured in a cup which was used as the container in the experiments. The container was kept on the workbench and the F theta lens was set 125 mm distance over the sludge surface so that the focal point was adjusted on the material surface. Laser beam was focused on top of the surface of the sludge. For the initial experiment, the focal point was 0, on the surface of the material. The position of the lens was controlled, and the distance was varied from the material surface to change the focal positions. The laser treatment process was run for every different parameter values' setup on the sludge surface for a 30mm*30mm square area. The laser device was operated by the software and the hatch spacing and scanning speed were varied. Power of the laser was controlled and set to maximum average power 20 W.

The formation of plasma was examined using a Spectrometer. The spectrometer was connected to the scanner head through its optical fiber. For every experiment, the software recorded the result soon after the ending of treatment of the designated scanning area. The data converter processed the measurements of the spectral intensity of the plasma and converted into numerical value. The converter was connected to the computer and the numerical data were recorded in the software. During the experiment, the laser beam moved forward in a straight direction. To measure continuous emission of the plasma cloud, the measuring head was set stationary in front of the beam.

3.5 Parameters

The primary parameters for the experimental setup were selected based on a visual observation. Visually observable strongest plasma was formed for the parameters mentioned in the table. Focal point position, overlap and processing speed were varied in further experiments. These parameters were set in the laser device as the initial experimental setup.

Table 3. Primary parameters used in the experimental setup

Pulse duration, ns	Scanning Speed, mm/s	Input power, W	Overlap, %	Focal point position, mm	Frequency, kHz	Hatch spacing, mm
50	400	20	50	0	20	0.03

Hatch spacing is the measurement of space between two consecutive lines of beam movement.

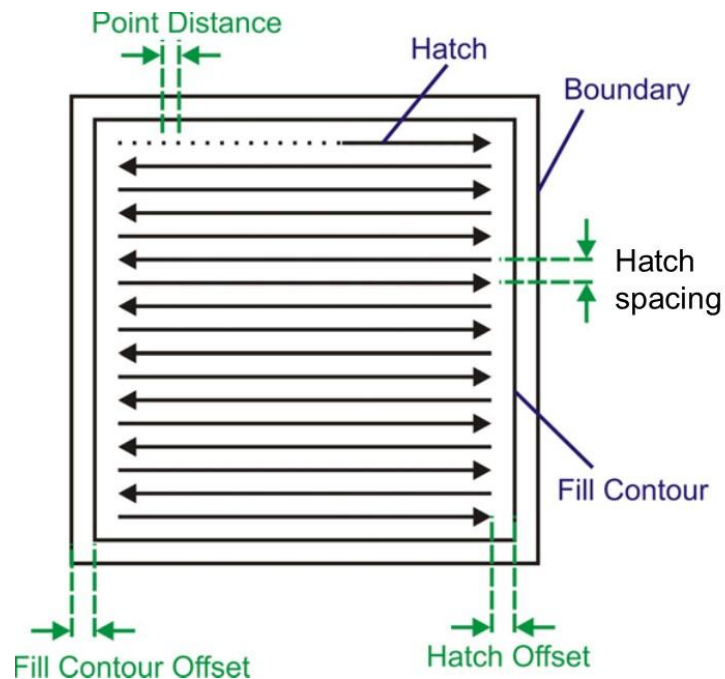


Figure 12. Hatch spacing between the beam scan paths

Frequency denotes the pulse repetition rate of the laser beam, which is the number of pulses per time unit. Scanning speed is the set value of the beam's movement in a straight line per time unit. The beam was guided to scan a total area of 30 mm * 30 mm for each of the parameter combination. Output power of the pulse in pulsing remains higher than half of the maximum for a certain period for every pulse and that is defined as the pulse duration. Laser beam power was 20 W and the pulse repetition frequency was 20 kHz. Therefore, the output energy per pulse was 20W/20000Hz, equivalent to 1mJ.

Beam overlap is the measurement of the convergence of the two consecutive spots' edges. Figure 11 shows in a marked area - the overlap of two consecutive spots. $R_{\text{overlap}} = 1 - x/D$ and $x=v/f$, where, D is the spot size of the beam, f is the laser pulse repetition frequency and v are the scanning speed (Marczak 2015, p. 2221-2234).

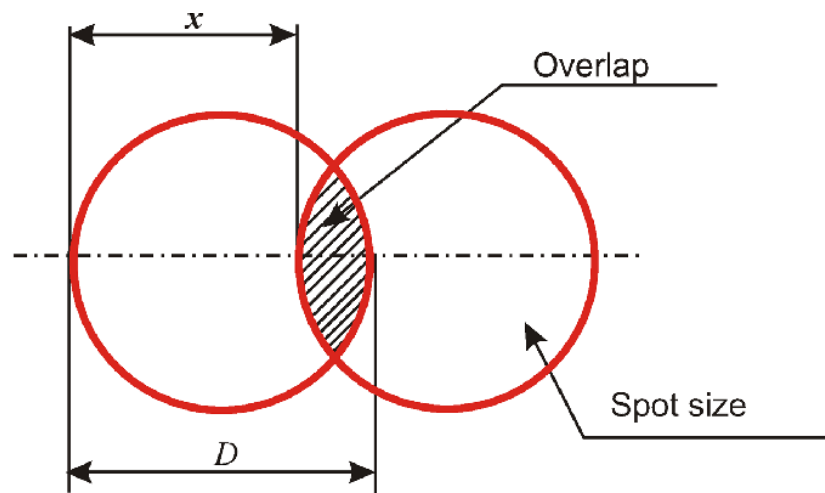


Figure 13. Overlap of laser beam (Marczak 2015, p. 2221-2234).

Table 4. Parameters for the variations in focal point position

Pulse duration, ns	Scanning speed, mm/s	Power, W	Frequency, kHz	Hatch spacing, mm	Focal point position
50	400	20	20	0.03	+3.5
					+3.0
					+2.5
					+2.0
					+1.5
					+1.0
					+0.5
					0.0
					-0.5
					-1.0
					-1.5
					-2.0
					-2.5
					-3.0
					-3.5

Table 5. Parameters for the variations in processing speed

Pulse duration, ns	Power, W	Focal point position, mm	Frequency, kHz	Hatch, mm	Processing speed, mm/s
50	20	0	20	0.03	200
					300
					400
					500
					600

Table 6. Parameters for the variations in hatch spacing

Pulse duration, ns	Processing speed, mm/s	Power, W	Overlap, %	Focal point position, mm	Frequency, kHz	Hatch spacing, mm
50	400	20	50	0	20	0.01
						0.02
						0.03
						0.04
						0.05
						0.06

4 RESULTS

4.1 Effect of the focal point positions

Fifteen different focal point positions were tested during the experiments within a range of -3.50 mm to +3.50 mm. The focal point position was changed with an interval of 0.5 mm; the 0 position was defined to be on top of the surface of the sludge.

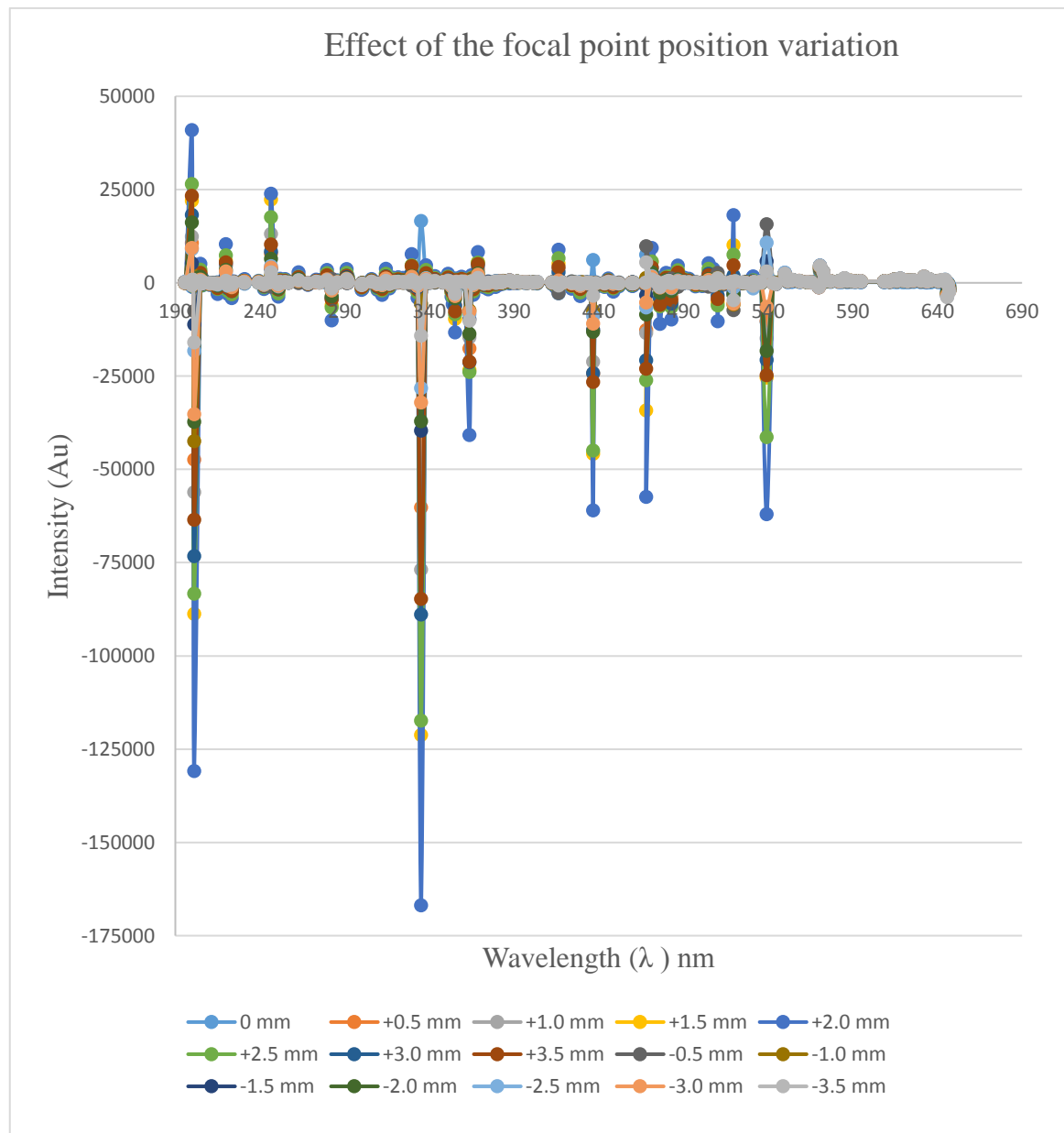


Figure 14. Comparison of spectral intensity of plasma during focal point position variation

The spectral intensity of plasma varied due to the variation in focal point position variation. It can be seen from the graphical representation that the highest values were recorded for +2.0 mm focal point position. The overall spectral intensity increased gradually when moving from 0 mm to +2.0 mm position, decreasing again as value of focal point position kept increasing. For negative value of focal point position, the graph lines did not show high peak values.

The variations in focal point position effected the spot diameter of the laser beam on surface of the material. The diameter of the beam at focal point position was 40 μm and the input energy was 1 mJ. When the focal point position was moved to a positive value direction, the path length between biosludge and the lens increased.

4.2 Effect of the scanning speed

Five different scanning speed were investigated from 200 mm/s to 600 mm/s with an interval of 100 mm.

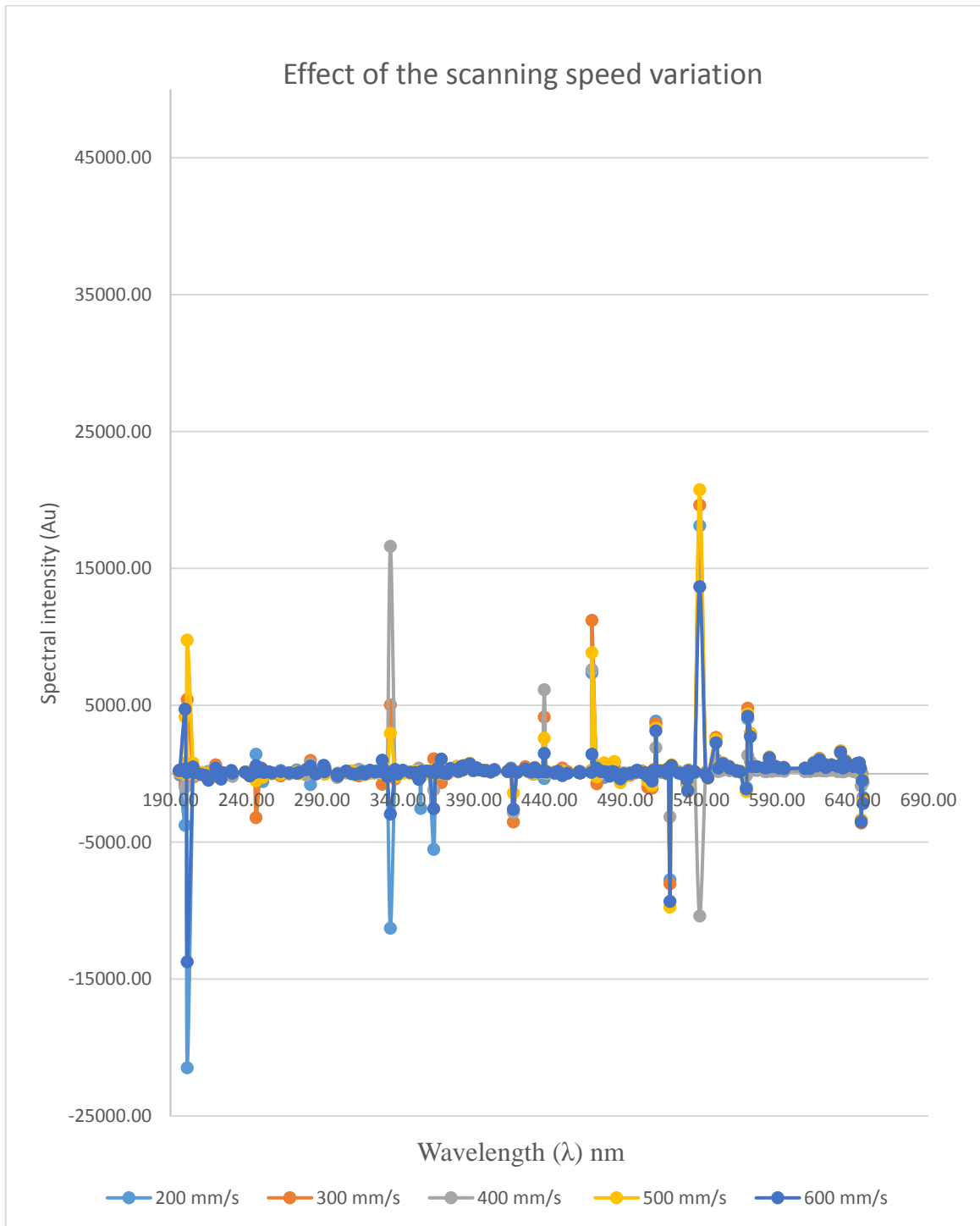


Figure 15. The comparison of spectral intensity of plasma during scanning speed variation

Spectral intensity value of plasma varied due to the variation in scanning speed variation. Top peak value was recorded at the lowest speed, for the scanning speed of 200 mm/s. During the processing speed variation, the focal point position was constant at 0 mm, so the spot diameter of laser beam was equal to the laser beam diameter at focal point and it was kept same for every experiment.

$R_{\text{overlap}} = 1 - x/D$ and $x=v/f$, where, D is the spot size of the beam, f is the laser pulse repetition frequency and v are the scanning speed (Marczak 2015, p. 2221-2234). The pulse repetition frequency f was 20 kHz and the spot size (beam diameter) of the laser beam D was 40 μm .

When, processing speed v was 200 mm/s, $x= 10$ and $R_{\text{overlap}}=75.0\%$.

When, processing speed v was 300 mm/s, $x= 10$ and $R_{\text{overlap}}=62.5\%$.

When, processing speed v was 400 mm/s, $x= 10$ and $R_{\text{overlap}}=50.0\%$.

When, processing speed v was 500 mm/s, $x= 10$ and $R_{\text{overlap}}=37.5\%$.

When, processing speed v was 600 mm/s, $x= 10$ and $R_{\text{overlap}}=25.0\%$.

Overlap percentage of beam is inversely proportionated to processing speed. Overlap ratio decreases with the increases of the processing speed if the beam diameter and hatch spacing are kept constant. From the graphical presentation, the values showed the effect of overlap percentage on the spectral intensity of plasma. Higher overlap ratio and higher energy density created brighter plasma.

Energy density, $E= P / v \times h$, where P is the effective laser power, v is the scanning speed and h is the hatch spacing (Carter 2016, p. 657-661). While varying processing speed, the effective laser power 20 W and the hatch spacing 0.03 mm were kept constant. So, the lower processing speed created higher energy density in the scanning area.

Energy density at 200 mm/s scanning speed was 3.33 J/mm² or 3.33 $\mu\text{J}/\mu\text{m}^2$

Energy density at 300 mm/s scanning speed was 2.22 J/mm² or 2.22 $\mu\text{J}/\mu\text{m}^2$

Energy density at 400 mm/s scanning speed was 1.67 J/mm² or 1.67 $\mu\text{J}/\mu\text{m}^2$

Energy density at 500 mm/s scanning speed was 1.33 J/mm² or 1.33 $\mu\text{J}/\mu\text{m}^2$

Energy density at 600 mm/s scanning speed was 1.11 J/mm² or 1.11 $\mu\text{J}/\mu\text{m}^2$

4.3 Effect of the hatch spacing

Six different hatch spacing were experimented with spacing between the lines from 0.01 mm to 0.06 mm using an interval of 0.01 mm.

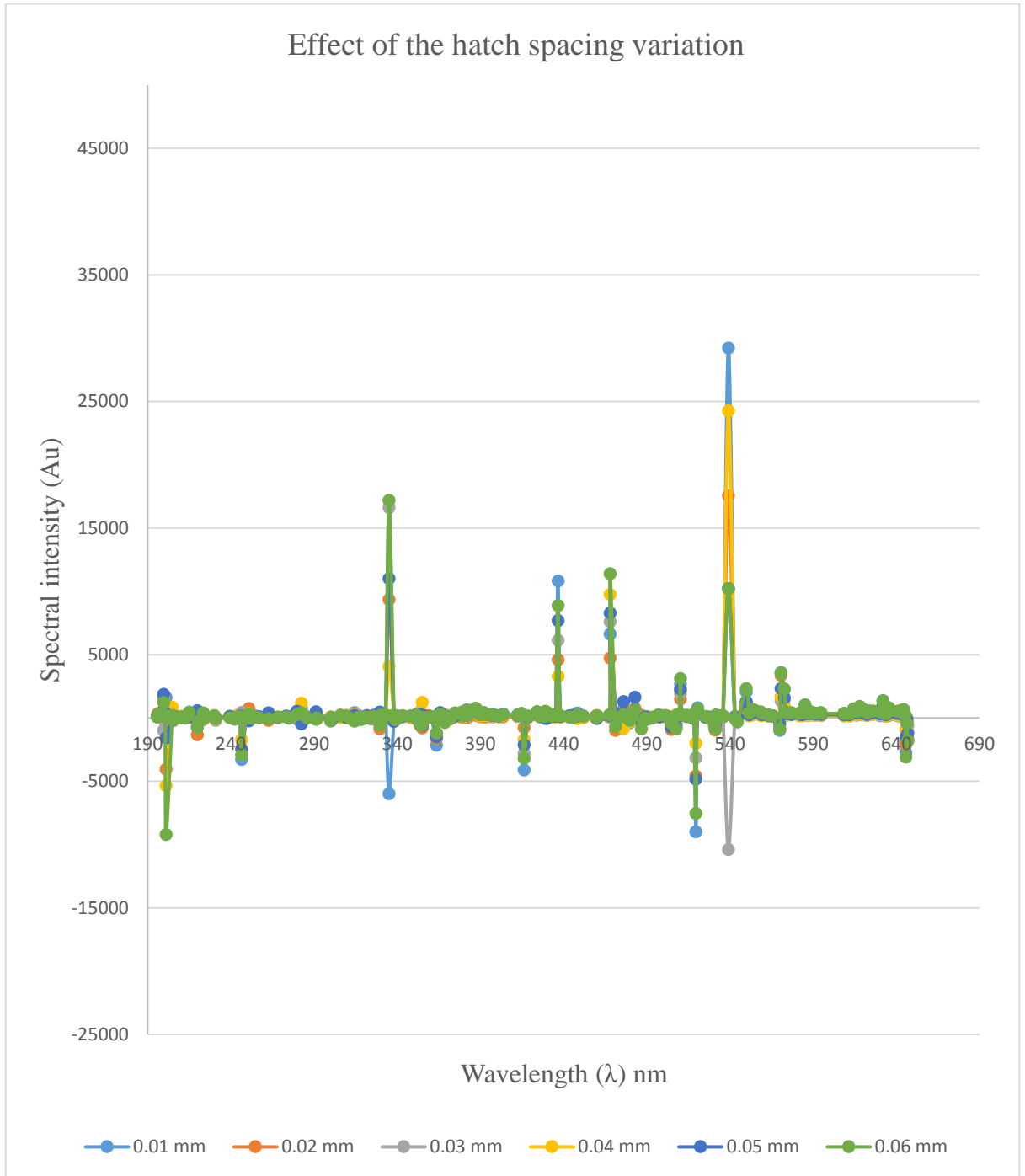


Figure 16. The comparison of spectral intensity of plasma with different hatch spacing values.

Spectral intensity varied due to the hatch spacing variation. Top peak was recorded for the lowest hatch spacing of 0.03 mm. During the hatch spacing variation, the focal point position was constant at 0 mm, so the spot diameter of laser beam was equal to the laser beam diameter at focal point and it was kept same for every experiment. The effective laser power of 20 W and scanning speed at 400 mm/s were kept constant during the tests with hatch spacing variation.

From the equation of energy density, $E = P / v \times h$, where P is the effective laser power, v is the scanning speed and h is the hatch spacing (Carter 2016, p. 657-661), the hatch spacing effected the energy density inversely proportional.

For hatch spacing 0.01 mm, Energy density, $E = 5.00 \text{ J/mm}^2$ or $5.00 \text{ } \mu\text{J/} \mu\text{m}^2$

For hatch spacing 0.02 mm, Energy density, $E = 2.50 \text{ J/mm}^2$ or $2.50 \text{ } \mu\text{J/} \mu\text{m}^2$

For hatch spacing 0.03 mm, Energy density, $E = 1.67 \text{ J/mm}^2$ or $1.67 \text{ } \mu\text{J/} \mu\text{m}^2$

For hatch spacing 0.04 mm, Energy density, $E = 1.25 \text{ J/mm}^2$ or $1.25 \text{ } \mu\text{J/} \mu\text{m}^2$

For hatch spacing 0.05 mm, Energy density, $E = 1.00 \text{ J/mm}^2$ or $1.00 \text{ } \mu\text{J/} \mu\text{m}^2$

For hatch spacing 0.06 mm, Energy density, $E = 0.83 \text{ J/mm}^2$ or $0.83 \text{ } \mu\text{J/} \mu\text{m}^2$

5 DISCUSSIONS & CONCLUSIONS

The wavelength of the laser used in the experiments was 1064 nm. Plasma formation was compared using a spectrometer to record the effect of the changes in parameters on plasma intensity. The spectral intensity of the plasma was recorded and plotted in graphs corresponding to wavelength. The spectrometer recorded intensity values among 190 nm to 640 nm wavelength range. The higher value of spectral intensity from the plasma indicated the formation of brighter plasma. In result graphs, top peaks were also recorded in the negative direction because in the experimental setup the reflectance monitor of spectrometer was set in front of the beam source.

Change of focal point position effected the spot diameter of the laser beam on surface and therefore also energy density delivered to certain area. The threshold energy varied in different locations in material because of the water percentage ratio in the materials. The lowest threshold energy was on the sludge surface, so the brightest plasma was formed when the beam interacted with the sludge particles. When the scanning speed was decreased, keeping the focal position and hatch spacing constant, the energy density per unit area continuously increased. From the spectral intensity graph, the lowest scanning speed created the brightest plasma due to the higher energy density. If the scanning speed is increased to a very high rate, after a certain level, the energy density is much lower than the required threshold energy. In this study, after 400 mm/s scanning speed, for higher processing speed, the graph lines showed the same pattern and did not show any top peak values. Hatch spacing effected the energy density and lower hatch spacing brought more energy in certain area. The threshold energy varied in different locations in materials and effected the results of the experiments. Laser energy less than the threshold energy did not show spectral intensity in the graphs. The experiment showed the tendency of plasma to be brighter with higher energy density. The parameter setup was effective in which the energy density exceeded the lowest required threshold energy of 1.8 μJ . Low hatch spacing and low scanning speed found to be effective for high energy density and the optimum interaction point of beam and materials with the lowest threshold energy on sludge surface created the brightest plasma.

6 FUTURE WORK RECOMMENDATIONS

Cell lysis using laser beam should be studied using laser sources capable to produce higher peak power since initiating the cavitation bubble requires higher pulse energies than equipment used in this study was capable to produce. Alternatively, lasers emitting at shorter wavelengths could be applied to study the plasma formation.

REFERENCES

- Brown, R.B. and Audet, J., 2008. Current techniques for single-cell lysis. *Journal of the Royal Society Interface*, 5(Suppl 2), pp. S131-S138.
- Carter, L.N., Wang, X., Read, N., Khan, R., Aristizabal, M., Essa, K. and Attallah, M.M., 2016. Process optimisation of selective laser melting using energy density model for nickel-based superalloys. *Materials Science and Technology*, 32(7), pp.657-661.
- Dhawan, M.D., Wise, F. and Baeumner, A.J., 2002. Development of a laser-induced cell lysis system. *Analytical and bioanalytical chemistry*, 374(3), pp.421-426.
- Gazor, M., Talesh, S.S.A., Khatami, M., Javidanbardan, A. and Hosseini, S.N., 2018. A Novel Cell Disruption Approach: Effectiveness of Laser-induced Cell Lysis of *Pichia pastoris* in the Continuous System. *Biotechnology and Bioprocess Engineering*, 23(1), pp.49-54.
- Glezer, E.N., Schaffer, C.B., Nishimura, N. and Mazur, E., 1997. Minimally disruptive laser-induced breakdown in water. *Optics letters*, 22(23), pp.1817-1819.
- Hellman, A.N., Rau, K.R., Yoon, H.H. and Venugopalan, V., 2008. Biophysical Response to Pulsed Laser Microbeam-Induced Cell Lysis and Molecular Delivery. *Journal of biophotonics*, 1(1), pp.24-35.
- IPG Laser GmbH. (2009). *Specification Ytterbium Pulsed Fiber Laser*, YLPM-1-4x200-20-20, Massachusetts, USA, Available in pdf file: www.sunpump.com.cn/UploadFile/2015-8/YLPM-20W.pdf

Jadhav, S.V., Haramkar, S.S., Kamble, A.R. and Thorat, B.N., 2017. Insights into dewatering and characterization of the waste activated sludge. *Journal of the Taiwan Institute of Chemical Engineers*, pp. 1-7.

Lai, H.H., Quinto-Su, P.A., Sims, C.E., Bachman, M., Li, G.P., Venugopalan, V. and Allbritton, N.L., 2008. Characterization and use of laser-based lysis for cell analysis on-chip. *Journal of The Royal Society Interface*, 5(Suppl 2), pp. S113-S121.

Lauterborn, W. and Vogel, A., 2013. Shock wave emission by laser generated bubbles. In *Bubble dynamics and shock waves* (pp. 67-103). Springer, Berlin, Heidelberg.

Lin, C.P., Kelly, M.W., Sibayan, S.A., Latina, M.A. and Anderson, R.R., 1999. Selective cell killing by microparticle absorption of pulsed laser radiation. *IEEE Journal of selected topics in quantum electronics*, 5(4), pp.963-968.

Marczak, J., 2015. Micromachining And Patterning In Micro/Nano Scale On Macroscopic Areas. *Archives of Metallurgy and Materials*, 60(3), pp.2221-2234.

McMillan, J.R., Watson, I.A., Ali, M. and Jaafar, W., 2013. Evaluation and comparison of algal cell disruption methods: microwave, waterbath, blender, ultrasonic and laser treatment. *Applied energy*, 103, pp.128-134.

Mittal, K.L. and Lei, W.S. eds., 2018. *Laser Technology: Applications in Adhesion and Related Areas*. John Wiley & Sons, p. 401.

Mowla, D., Tran, H.N. and Allen, D.G., 2013. A review of the properties of biosludge and its relevance to enhanced dewatering processes. *Biomass and Bioenergy*, 58, pp.365-378.

Negi, S. and Sharma, R.K., 2015. Influence of Processing Variables on Dynamic Mechanical Response of Laser-Sintered Glass-Filled Polyamide. *Materials and Manufacturing Processes*, 30(12), pp.1431-1441.

Nishio, M., Maruko, A., Inoue, M., Takama, M., Matsubara, S., Okunishi, H., Kato, K., Kyomoto, K., Yoshida, T., Shimabayashi, K. and Morioka, M., 2014, September. High-efficiency cavity-dumped micro-chip Yb: YAG laser. In *Pacific Rim Laser Damage 2014: Optical Materials for High-Power Lasers* (Vol. 9238, p. 92380K). International Society for Optics and Photonics.

Ocean Optics, Inc. *HR2000+ and HR2000+CG-UV-NIR Series - High-Resolution Fiber Optic Spectrometers Installation and Operation Manual*, Document Number 294-00000-000-02-0705, Available at: <https://oceanoptics.com/wp-content/uploads/hr2000-.pdf>

Rau, K.R., Guerra III, A., Vogel, A. and Venugopalan, V., 2004. Investigation of laser-induced cell lysis using time-resolved imaging. *Applied Physics Letters*, 84(15), pp.2940-2942.

Rau, K.R., Quinto-Su, P.A., Hellman, A.N. and Venugopalan, V., 2006. Pulsed laser microbeam-induced cell lysis: time-resolved imaging and analysis of hydrodynamic effects. *Biophysical journal*, 91(1), pp.317-329.

Schaffer, C.B., Nishimura, N., Glezer, E.N., Kim, A.M.T. and Mazur, E., 2002. Dynamics of femtosecond laser-induced breakdown in water from femtoseconds to microseconds. *Optics express*, 10(3), pp.196-203.

Shehadul Islam, M., Aryasomayajula, A. and Selvaganapathy, P., 2017. A review on macroscale and microscale cell lysis methods. *Micromachines*, 8(3), p.83.

Silfvast, W.T., 1996. *Laser Fundamentals* Cambridge University Press. New York, NY, p.53-59.

Sklar, L.R., Burnett, C.T., Waibel, J.S., Moy, R.L. and Ozog, D.M., 2014. Laser assisted drug delivery: a review of an evolving technology. *Lasers in surgery and medicine*, 46(4), pp.249-262.

spie.org, (2008). *SPIE's official website*. [online] Available at: https://spie.org/publications/fg14_p01-04_optical_pulses?SSO=1 / [Accessed: 17 June. 2018].

Theory.labster.com, *Lysis – Labster Theory*. [Online] Available at: <https://theory.labster.com/lysis/> [Accessed: 21 August 2018].

Venugopalan, V., Guerra III, A., Nahen, K. and Vogel, A., 2002. Role of laser-induced plasma formation in pulsed cellular microsurgery and micromanipulation. *Physical review letters*, 88(7), p.078103.

Vogel, A., Nahen, K., Theisen, D. and Noack, J., 1996. Plasma formation in water by picosecond and nanosecond Nd: YAG laser pulses. I. Optical breakdown at threshold and superthreshold irradiance. *IEEE Journal of Selected Topics in Quantum Electronics*, 2(4), pp.847-860.

Wang, J.L. and Xu, L.J., 2012. Advanced oxidation processes for wastewater treatment: formation of hydroxyl radical and application. *Critical Reviews in Environmental Science and Technology*, 42(3), pp.251-325.

Watanabe, W., Matsunaga, S., Shimada, T., Higashi, T., Fukui, K. and Itoh, K., 2005. Femtosecond laser disruption of mitochondria in living cells. *Medical Laser Application*, 20(3), pp.185-191.

Wu, T., Yu, X., Hu, A., Zhang, L., Jin, Y. and Abid, M., 2015. Ultrasonic disruption of yeast cells: Underlying mechanism and effects of processing parameters. *Innovative Food Science & Emerging Technologies*, 28, pp.59-65.

Yin, X., Han, P., Lu, X. and Wang, Y., 2004. A review on the dewaterability of bio-sludge and ultrasound pretreatment. *Ultrasonics sonochemistry*, 11(6), pp.337-348.